Strengthening of RC Deck Slabs by High-Fiber-Density CFRP

Hwakian Chai*, Hiroshi Ohnishi**, Shigeyuki Matsui***

*M. of Eng, Dept. of Civil Eng., Osaka University, Yamadaoka, Suita, Osaka 565-0871

**M. of Eng, Assistant Prof., Dept. of Civil Eng., Osaka University, Yamadaoka, Suita, Osaka 565-0871

***Dr. of Eng., Prof., Dept of Civil Eng., Osaka University, Yamadaoka, Suita, Osaka 565-0871

Bond behavior and strengthening performance of two types of high-fiber-density CFRP sheets, namely the laminated type and warp-knitted type are investigated. Comparison between applying single layer of the high-fiber-density CFRP sheet and double layers of the CFRP sheets with lower fiber density in strengthening of RC slabs of highway bridge decks is also carried out. Results based on the CFRP-concrete bond tests and the fatigue tests for full-scale slab specimens are presented. Generally, the warp-knitted type CFRP sheet is found to be equally effective as the laminated type CFRP sheet in strengthening the RC slabs. In addition, by bonding single layer of high-fiber-density CFRP sheet, the strengthening performance does not decrease from that of bonding double layers of CFRP sheets with lower fiber density.

Keywords: bond behavior, fatigue durability, high-fiber-density CFRP sheets, strengthening

1. Introductions

Since a decade ago, research and development on the strengthening of deteriorated reinforced concrete (RC) slabs of highway bridge decks by carbon fiber reinforced plastic (CFRP) sheets have been carried out. Previous studies [1)-4)] indicate that CFRP sheets with reasonably high elastic modulus (approximately 400GPa and above) are highly effective in extending the fatigue lifespan of RC slabs subjected to traffic load. Because one of the most important parameters that affect the strengthening performance is the tensile stiffness, which is determined by the elastic modulus and unit cross sectional area of CFRP sheet, it is considered that similar strengthening effect can be achieved by employing CFRP sheets of lower elastic modulus but higher amount of carbon fiber per unit which produces higher cross sectional thickness. By adopting this class of CFRP sheets, namely the high-fiber-density CFRP sheets, lower cost and shorter executing time when compared with bonding several equivalent layers of CFRP sheets of lower fiber densities can be achieved. Also, better performance of the strengthening work can be expected.

It is known that in the strengthening of RC members by bonding FRP composites, composite action of transferring of stresses from the concrete substrate to the FRP composites is

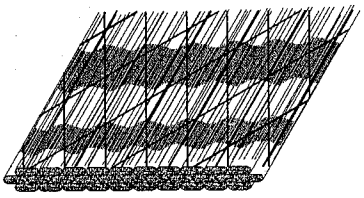

(a) Laminated type

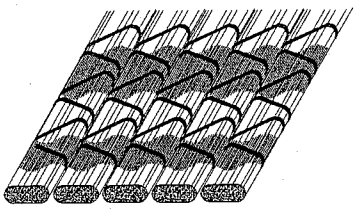

(b) Warp-knitted type

Fig. 1 Types of CFRP sheet

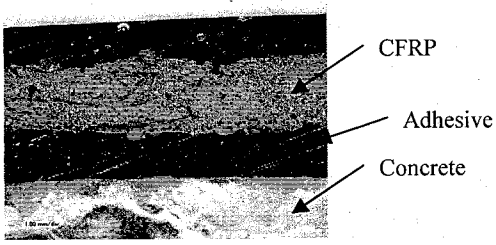

(i) Laminated structure

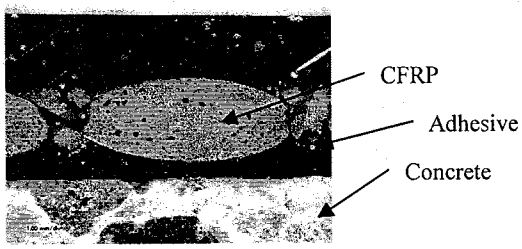

(ii) Warp-knitted structure

Fig. 2 Cross sectional image of CFRP-concrete bond

usually developed within an adhesive layer such as epoxy resin. Thus, the bond behavior is one of the factors that dominate the effectiveness of the strengthening method. With this inference, it is essential to investigate the interfacial stresses as well as the bond strength and durability to verify the overall strengthening performance.

In this research, evaluation of the bond behavior and strengthening performance of the high-fiber-density CFRP sheets is carried out. Two types of CFRP sheets with different knit structures, namely a conventional laminated structure and a relatively new warp-knitted structure (Fig.1), were investigated. The warp-knitted CFRP sheet was developed to improve the bond between the concrete and the CFRP sheet due to better penetration of epoxy resin between bundles of wrapped carbon fibers as shown in Fig. 2.

In the experimental program, the strength and durability of CFRP-concrete bond are investigated by bond tests. A new testing instrument was developed to serve the purposes. Besides, fatigue tests on full-scale RC slab specimens were also conducted by using the wheel running machine to study the performance of the CFRP sheets in extending the fatigue lifespan of slabs.

2. CFRP-concrete bond tests

A new testing instrument was developed in Osaka

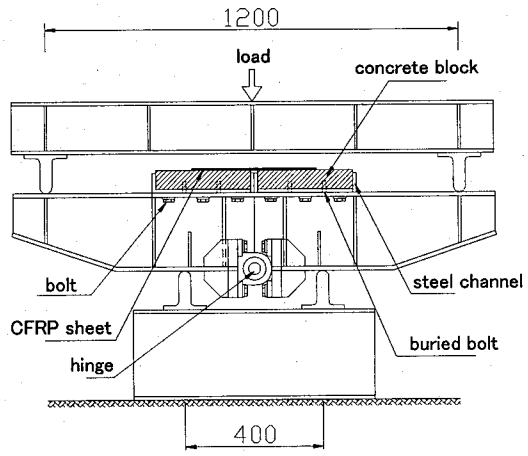

Fig. 3 Instrument for bond test

University to evaluate the strength of the CFRP-concrete bond and to clarify the debonding phenomenon of the CFRP sheets under fatigue loading. Fig. 3 shows the schematic diagram of the testing instrument. The CFRP sheet was bonded to the top surfaces of two separate concrete blocks, which were fixed to two separate H-shape steel girders. The steel girders were connected to each other by a hinge at the lower part. Load was applied at the center of the loading beam and was transferred to the edges of the steel girders below. The distance between the two loading positions was 1200mm and the distance between the two supports was 400mm. When the load was applied, the girders displaced and an opening between the girders was created, which induced normal stress to the CFRP sheets and then generated shear stress in the adhesive layer between the

CFRP sheet and the concrete blocks. Repeated acts of loading and unloading simulated the opening-closing movements of cracks in a concrete slab that caused pulsating shear stress to the adhesive layer.

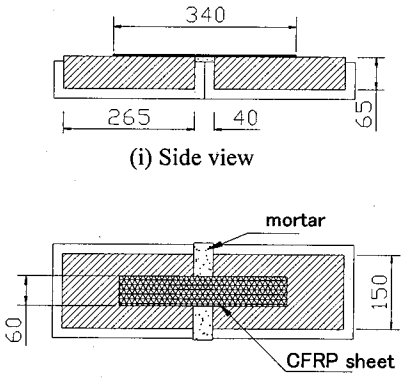

(i) Side view

(ii) Plan view

Fig. 4 Specimen layout

2.1 Specimen details and Instrumentations

Fig. 4 shows the layout of the specimens. Each specimen consisted of two 265 x 150 x 65mm concrete blocks joined up by bonding CFRP sheet on the top surfaces. The blocks were fixed to a steel channel by buried bolts, respectively, and the steel channels were connected to the steel girder flange by another set of bolts as shown in Fig. 3. A gap of 40mm between the blocks was filled with mortar.

Two sets of specimens were prepared and tested. Specimens in set L300*2 were bonded with two layers of unidirectional 300g/m^2 laminate type CFRP sheets in longitudinal direction of specimens. On the other hand, specimens in set W600 were bonded with one layer of unidirectional 600g/m^2 warp-knitted type CFRP sheets. Four specimens were prepared for each set, in which two specimens were tested under static load and the remaining two were tested under fatigue load, respectively. Details of the specimens and the properties of the CFRP sheets are presented in Table 1.

Strain measurements were carried out in both the static and fatigue load tests. Fig. 5 shows the position of strain gages. The strain gages were arranged in two rows along the longitudinal directions of the CFRP sheet. It is noted that strain gage A8 was located at the longitudinal center of the CFRP sheet.

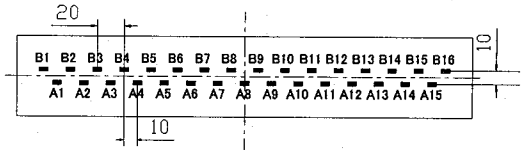

Fig. 5 Strain gage position

2.2 Test methods

In the static load test, the main objective was to investigate the bond strength of the CFRP sheets to concrete. Static load was applied and increased gradually until discontinuity of the specimens occurred due to failure of bond between the concrete substrate and the CFRP sheets at either one of the two concrete blocks of each specimen. For fatigue load test, repeated loading was applied with a frequency of 3Hz. The loading was conducted at two different ranges. Specimens L300*2-c and W600-c were loaded with repeated load with a maximum and a minimum magnitudes of 22kN and 2kN, while L300*2-d and W600-d were subjected to the maximum and the minimum repeated load of 26kN and 2kN, respectively. Fatigue test were terminated when the bond failure occurred.

Table 1 Bond test specimen details

Specimen	Test	CFRP sheet				
		Type	Fiber density (g/m^2)	Elastic modulus (GPa)	Design thickness (mm)	Tensile strength (MPa)
L300*2-a	static	laminated (high strength)	300	245	0.167	4160
L300*2-b	static					
L300*2-c	fatigue					
L300*2-d	fatigue					
W600-a	static	warp-knitted (high strength)	600	245	0.333	3400
W600-b	static					
W600-c	fatigue					
W600-d	fatigue					

2.3 Results and discussions

(i) Static load test

The bond failure in the static load tests was identified as debonding of CFRP sheets from the concrete surface. The debonding was caused by separation between the epoxy resin layer and the concrete substrate. Examples of the debonding of CFRP sheets are presented in Fig. 6. In the experiment, specimens L300*2-a and L300*2-b failed at 23.1kN and 33.1kN, respectively, while specimens W600-a and W600-b failed at 38.1kN and 34.0kN, respectively. The average load for the L300*2 and W600 specimens are 28.10kN and 36.05kN, respectively. The relations between load and strain at the center of the CFRP sheets are shown in Fig. 7. Both sets of specimens were considered to have similar volume of strengthening. Besides, the quantity of epoxy resin in the L300*2 specimens was actually two times that in the W600 specimens since the quantity was determined by the bonded area for each layer of CFRP sheet. It is suggested that the penetration rate of epoxy resin into the warp-knitted type CFRP sheet was higher compared to that of the laminated type CFRP sheets, which increased the effectiveness of distribution of stresses as well as the bond strength. Moreover, it is also suggested that a more complex interaction between the epoxy resin and the two layers

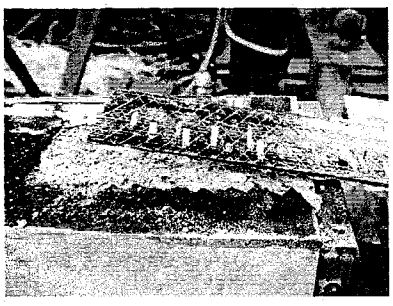

(i) L300*2-a

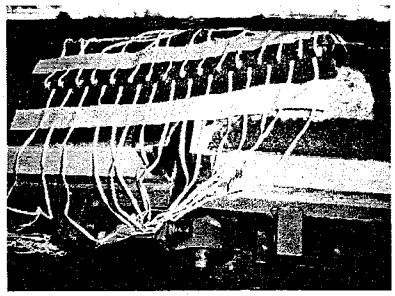

(ii) W600-a

Fig. 6 Debonding failure in static test

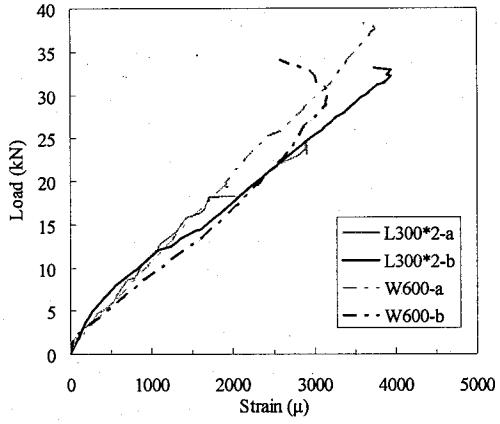

Fig. 7 Load-strain relation

of CFRP sheets as in the L300*2 specimens caused the distribution of stresses to become less effective compared to the W600 specimens. Further investigations in the interaction between the epoxy resin and CFRP sheets or concrete are therefore essential.

In the tests, it was observed that debonding initiated from the inner edge of one concrete block which was nearer to the gap between the two blocks. Debonding propagated towards the end of CFRP sheet. On the other hand, the bond remained sound for the other concrete block. Besides, it was noticed that failure of the bond between epoxy resin and concrete was the cause for the debonding. Ripping off of concrete from the surface of the specimens was also noticed. Since the gap between two concrete blocks of the specimens acted as 'flexural crack' when load was applied, the debonding can be considered as intermediate flexural crack-induced debonding.

For this type of debonding, Teng et. al.[5] suggested that when a major crack is formed, the tensile stress released by the concrete cracking is transferred to the CFRP sheet. As a consequent, high interfacial shear stress between the CFRP sheet and the concrete is induced near the crack. The interfacial shear stress increases with the applied load. When the stresses reach critical values, debonding is initiated at the crack and then propagates towards one of the sheet ends.

(ii) Fatigue load test

The total loading cycles to failure for specimens L300*2-c, L33*2-d and W600-d were approximately 9 x 105, 1 x 105 and

5 x 105 cycles, respectively. It is to be noted that W600-c did not fail after 3.0 x 10^6 cycles of fatigue load and the specimen was statically loaded to failure. Better bond performance by one layer of 600g/m^2 warp-knitted type CFRP sheet is verified when compared to the results of 2 layers of 300g/m^2 laminated type sheets under fatigue load. The progress of debonding, which was marked with an ink marker, is presented in Fig. 8. The debonding was caused by separation between epoxy resin layer and the CFRP sheet was observed in the experiment. In fact, the debonding was initiated from the inner edges of both concrete blocks of one specimen and expanded towards the respective sheet ends.

Fig. 9 shows the distribution of strain of the CFRP sheets at the maximum fatigue load. The distance between the two vertical dashed lines represents the distance of the CFRP sheets bonded to the mortar between two concrete blocks. The following are suggested: (1) At region outside the two dashed lines, debonding occurred at the location where the strains were almost similar to that at the region in between the two dashed lines. The boundaries of the debonding area are represented by arrows in Fig. 9. From the strain results, the debonding area of the W600 specimens seems to be smaller than that of the

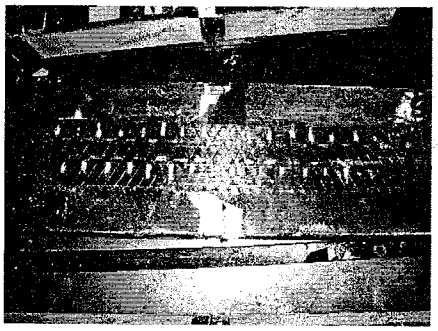

(i) L300*2-d

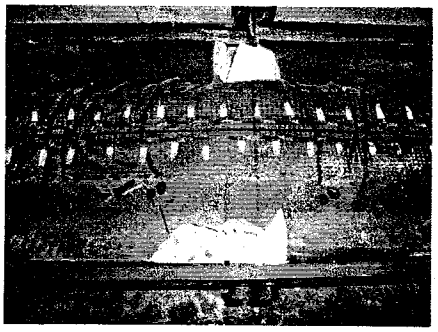

(ii) W600-c

Fig. 8 Debonding in fatigue test

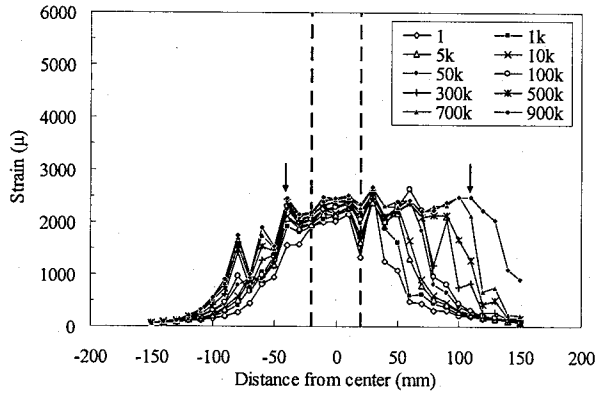

(i) L300*2-c

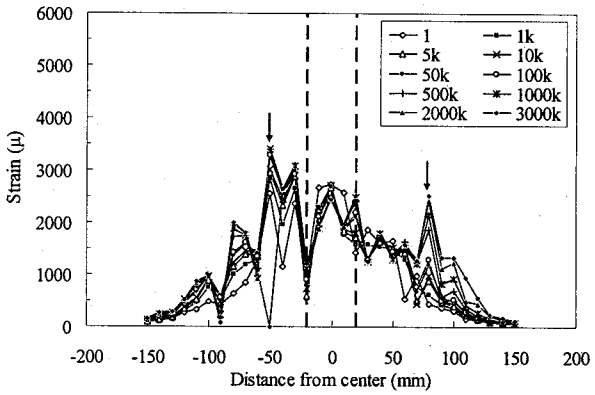

(ii) W600-c

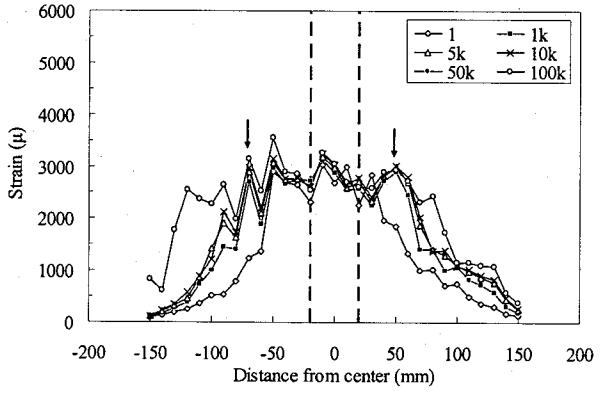

(iii) L300*2-d

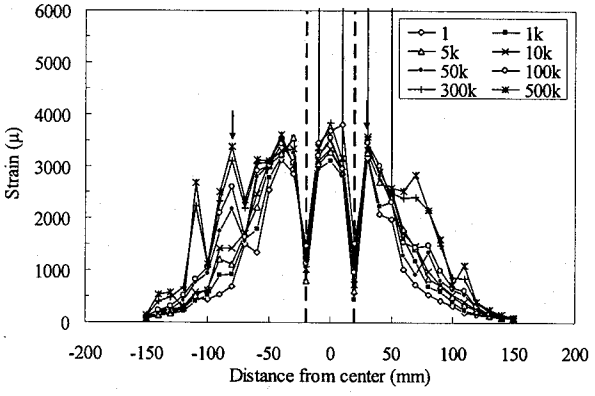

(iv) W600-d

Fig. 9 Strain distribution

L300*2 specimens at respective fatigue loading ranges, and (2) The strain of the W600 specimens were generally slightly higher than that of the L300*2 specimens especially at locations of debonding. The results were in agreement with that from the static load test, which suggest better transfer of stresses in specimen W600 compared to specimen L300*2, as well as less effective stress distributions by bonding 2 layers of CFRP sheets as in the L300*2 specimens.

2.4 Finite element analysis

It has been suggested that interfacial stresses dominates the debonding of CFRP sheets bonded to a cracked concrete subjected to static load [6)-7)]. Numerical analysis by finite element method (FEM) is thus carried out to study the influences of the type of CFRP sheets and the properties of adhesive layer on the CFRP-concrete bond behavior. By considering the symmetrical characteristics, only half of the specimen is modeled with appropriate boundary conditions. Fig. 10 illustrates the analytical model. Four-node plane stress element is used to model the steel girder, concrete block and adhesive layer. For CFRP sheet, truss element is implemented. The elastic modulus of concrete is taken as 35GPa. Besides that, the elastic modulus of epoxy resin is 5.30GPa for both types of CFRP sheets. It is assumed that under the actual loading, no deformation of steel girder occurred. Therefore in the analysis, the stiffness of the steel girder is considered to be very large and thus an infinite value is input for its elastic modulus. Because it is difficult to quantify the actual thickness of the adhesive layer, a uniform thickness of 0.5mm, which was based on an experimental estimation, is thus assumed in the analysis. Prefect bond between the concrete blocks and the epoxy resin, as well as between the epoxy resin and the epoxy resin, are assumed. Thus any forms of interfacial damages including cracks or yield are not considered.

Based on the strains distribution of CFRP sheets as shown in Fig. 11, good agreements between the analytical and experimental results can be obtained except that at higher loads the accuracy of the analytical model for 300g/m^2*2 CFRP sheets decreases. In fact, at higher loads the strains of the CFRP sheets in specimens L300*2 did not decrease with the measuring distance from the center. This phenomenon was probably due to the two adhesive layers and two CFRP sheets in the specimens, which caused the distribution of stresses to become complicated and less effective. Local debonding or defects which are not considered in the analytical model might have occurred in the actual tests.

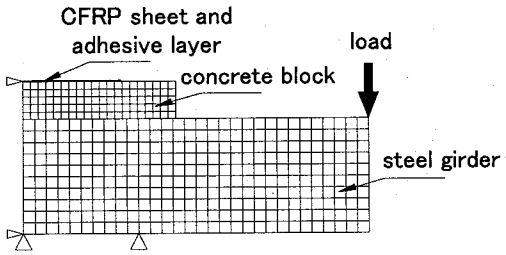

Fig. 10 FEM model

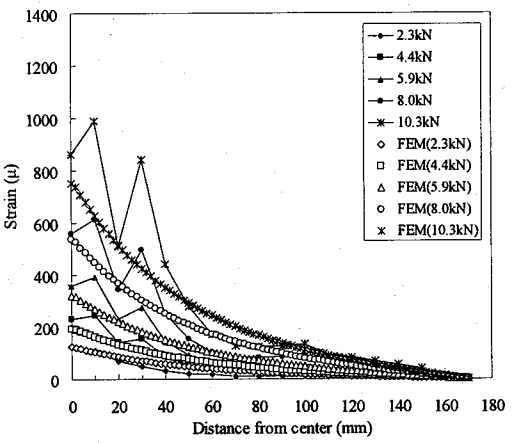

(i) 300g/m^2 * 2

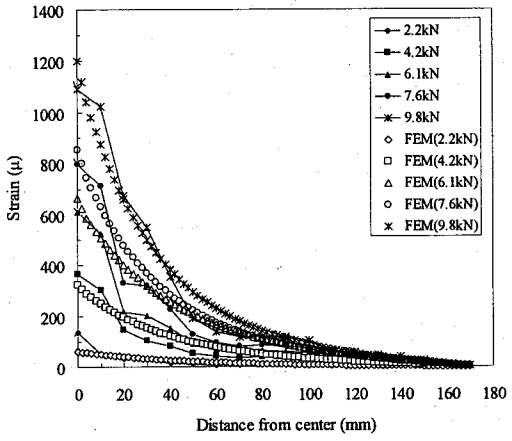

(ii) 600g/m^2

Fig. 11 Experimental and FEM strain results

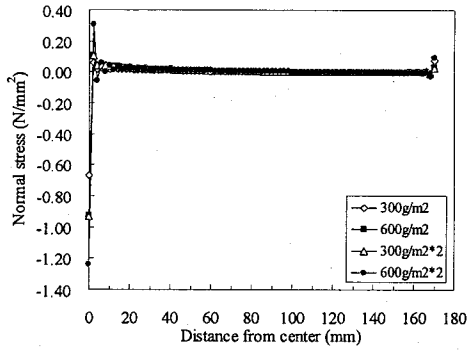

(i) Normal stress

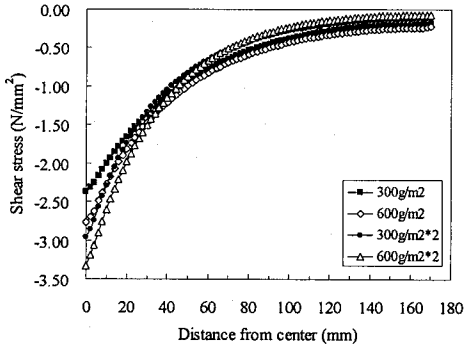

(ii) Shear stress

Fig. 12 Interfacial stresses

To investigate the stress distributions and for comparison purposes, models bonded with 300g/m^2 and 600g/m^2*2 CFRP sheets are also analyzed. The distribution of interfacial normal and shear stresses are shown in Fig. 12. High normal stress is concentrated at x = 0mm, which is also the position of the 'crack'. The maximum interfacial normal stress of models with 300g/m^2*2 and 600g/m^2 are very similar, nevertheless there is a more significant difference in interfacial shear stress between the two models. The interfacial stresses increase with the fiber density (thickness) as well as the number of layers of CFRP sheets. The interfacial shear stress of model with 300g/m^2*2 CFRP sheets becomes slightly higher than that with 600g/m^2 CFRP sheet at location near the 'crack'. It is probable that in the analysis, model with 300g/m^2*2 CFRP sheets are treated to have higher moment of inertia because of higher cross sectional thickness by adopting two adhesive layers.

By varying the elastic modulus of the adhesive, E_e, the distributions of interfacial shear stresses are studied (Fig. 13). Generally, with similar E_e, the interfacial shear stress in model with 600g/m^2 is higher than that of model with 300g/m^2*2 CFRP sheets. When E_e = 2.5GPa, interfacial shear stress for

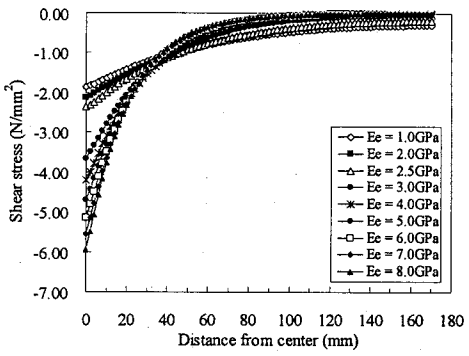

(i) 600g/m^2

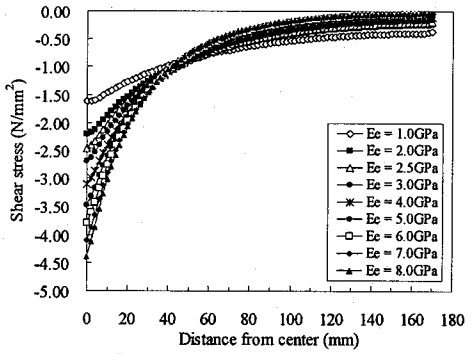

(ii) 300g/m^2*2 (adhesive in contact with concrete)

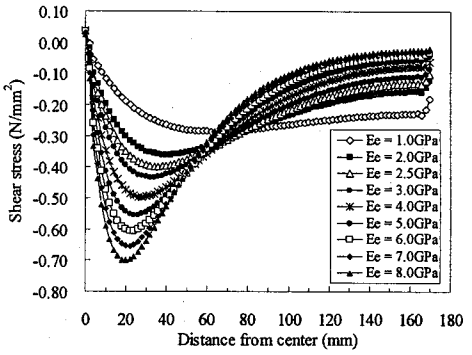

(iii) 300g/m^2*2 (adhesive between two CFRP sheets)

Fig. 13 Influence of E_e on interfacial shear stresses

models with 600g/m^2 and 300*2g/m^2 CFRP sheets are -2.37MPa and -2.47MPa, respectively. The interfacial shear stress increases when E_e increases. In model with 600g/m^2 CFRP sheet, a relatively significant increase in interfacial shear stress is noticed when E_e changes from 2.5GPa to 3.0GPa. In the model with 300g/m^2*2 CFRP sheets, the interfacial shear stress of adhesive layer, which is further from concrete substrate, are found to distribute in a different pattern. Furthermore, the maximum shear stress shifts towards the 'crack' when E_e increases. Besides that, the shear stress in adhesive layer closer to the concrete substrate increases with E_e, and a relatively significant increase is noticed when E_e increases from 1.0GPa to 2.0GPa.

3. Fatigue test by wheel running machine

To investigate the effectiveness of the high-fiber-density CFRP sheets in strengthening RC slabs of highway bridge decks, fatigue tests on full-scale specimens were carried out by using the wheel running machine. The testing machine simulates repeated moving wheel load similar to traffic load by heavy trucks on deck slabs. Accurate fatigue deterioration of deck slabs can thus be induced and the effect of strengthening by the CFRP sheets can be assessed.

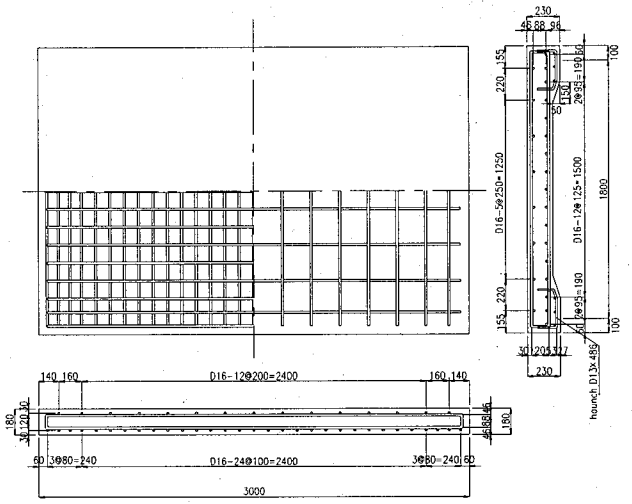

Fig. 14 Layout of slab specimen.

3.1 Specimens details and instrumentation

Fig. 14 shows the layout of the specimens. The specimens were models of actual deck slabs designed in accordance with the Japanese Specification for Highway Bridge Edition 1964. Six specimens with strengthening conditions as given in Table 2 were tested. All the specimens were designed with 28-day compressive strength of 24MPa. Properties of the concrete, measured during the course of the fatigue tests of respective specimens, are also presented in Table 2. The 300g/m^2 laminated type and 600g/m^2 warp-knitted type CFRP sheets have properties similar to that employed in the bond tests, as shown in Table 1. For 600g/m^2 laminated type CFRP sheet, the elastic modulus, tensile strength and design thickness are 253GPa, 4320MPa and 0.333mm, respectively. Tensile stiffness of the CFRP sheets, S_f is calculated by the following equation:

$$S_f = E_f t_f \quad (1)$$

where E_f and t_f are the elastic modulus and design thickness of the CFRP sheet, respectively. It is found that the specimens strengthened with the 300g/m^2*2 laminated type and 600g/m^2 warp-knitted type CFRP sheets have a S_f value of 81.6kN/m, whereas the specimens strengthened with the 600g/m^2 laminated type CFRP sheets yield a slightly higher S_f value of 84.2kN/m. It is to be noted that among the strengthened specimens, specimens W600D and W600D-H were subjected to the preliminary loading before the strengthening to simulate the deterioration condition of actual deck slabs. Besides, specimen W600D-H was designed to have concrete compressive strength and elastic modulus significantly higher than that of specimen W600D in order to investigate the influence of the concrete properties of deck slabs in the strengthening effect of CFRP sheets.

For the test set-up, all the deck slab specimens were supported simply along the longitudinal direction. Elastic support on the edges of slabs in the transverse directions was implemented by insertion of mortar layer into the gap between the specimens and the supporting cross beams. Loading programs for all the specimens are shown in Table 3.

Table 2 Details of slab specimens

Specimen	Strengthening condition	Preliminary loading	Concrete			
			Elastic modulus (GPa)	Compressive strength (MPa)	Tensile strength (MPa)	Poisson ratio
Control	unstrengthened	-	23.1	30.5	2.86	0.21
L300*2	300g/m^2 laminated CFRP	no	31.6	33.2	-	0.21
L600	300g/m^2 laminated CFRP	no	31.6	33.2	-	0.21
W600	600g/m^2 warp-knitted CFRP	no	25.5	30.7	2.85	0.23
W600D	600g/m^2 warp-knitted CFRP	yes	23.0	29.3	2.79	0.21
W600D-H	600g/m^2 warp-knitted CFRP	yes	35.8	41.0	2.29	0.20

Table 3 Loading Program

Specimen	No. of loading passages (x10^3)				
	Preliminary 150kN	150kN	170kN	180kN	210kN
Control	-	-	until fail	-	-
L300*2	-	100	-	700	until fail
L600	-	100	-	700	until fail
W600	-	100	-	700	until fail
W600D	30	100	-	700	until fail
W600D-H	30	100	-	700	until fail

Table 4 Total no. of loading passages, N_f

Specimen	No. of loading passages (x10^3)		
	preliminary loading	after strengthening	Total, N_f
Control[1)]	-	-	46
L300*2	-	950	950
L600	-	1,000[2)]	1,000
W600	-	804	804
W600D	30	954	984
W600D-H	30	1,398	1,428

[1)] Loaded until failure without strengthening
[2)] Did not fail and test was terminated

3.2 Experimental results

(i) Failure mode and total loading passages

After the preliminary loading, cracks were found on the tension surfaces of specimens W600D and W600D-H. The crack pattern and densities were very similar to that of the specimen Control, as illustrated in Fig. 15. For the strengthened specimens, all were loaded until failure except L600, which did not fail after 1,000,000 passages and the test was terminated. Fatigue failure similar to specimen Control occurred in all the strengthened specimens. Under repeated load, network of flexural cracks propagated on the tension surface of the slab. The flexural cracks then joint up with the transverse cracks initiated from the top surface of the slab caused by torsion moment. As results the slab loses its continuity as a plate and virtually transforms into several transverse concrete beams which were longitudinally distributed. At this time the stiffness of slab was greatly reduced and distribution of stresses became ineffective due to the discontinuity. Although opening-closing movements of cracks by flexure are restricted by the CFRP sheet, cracks that propagated in the longitudinal direction developed subsequently due to relative vertical movements of the cracks surfaces by shear.

The total loading passages, N_f inclusive of the preliminary loading passages are shown in Table 4. Specimen W600D has N_f higher than specimen W600 despite being subjected to preliminary loading. This was probably due to unanticipated defects of the specimen. More tests are thus required to verify

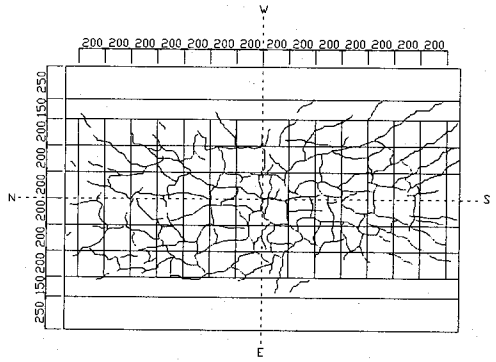

(i) W600D after preliminary loading

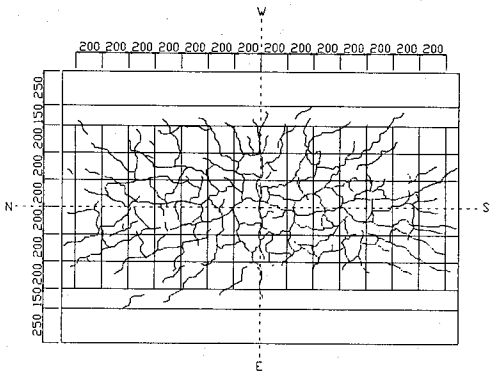

(ii) Control specimen at fatigue failure

Fig. 15 Cracks on tension surface

the results. For the other specimens, specimen W600D failed with N_f very close to that of specimen L300*2, whereas N_f of specimen W600D-H was significantly higher than that of specimen W600D. This indicated that fatigue durability of a deck slab is dominated by the concrete properties of the slab itself. Deck slabs that have better concrete properties are considered to be more durable compared to those with poorer concrete properties.

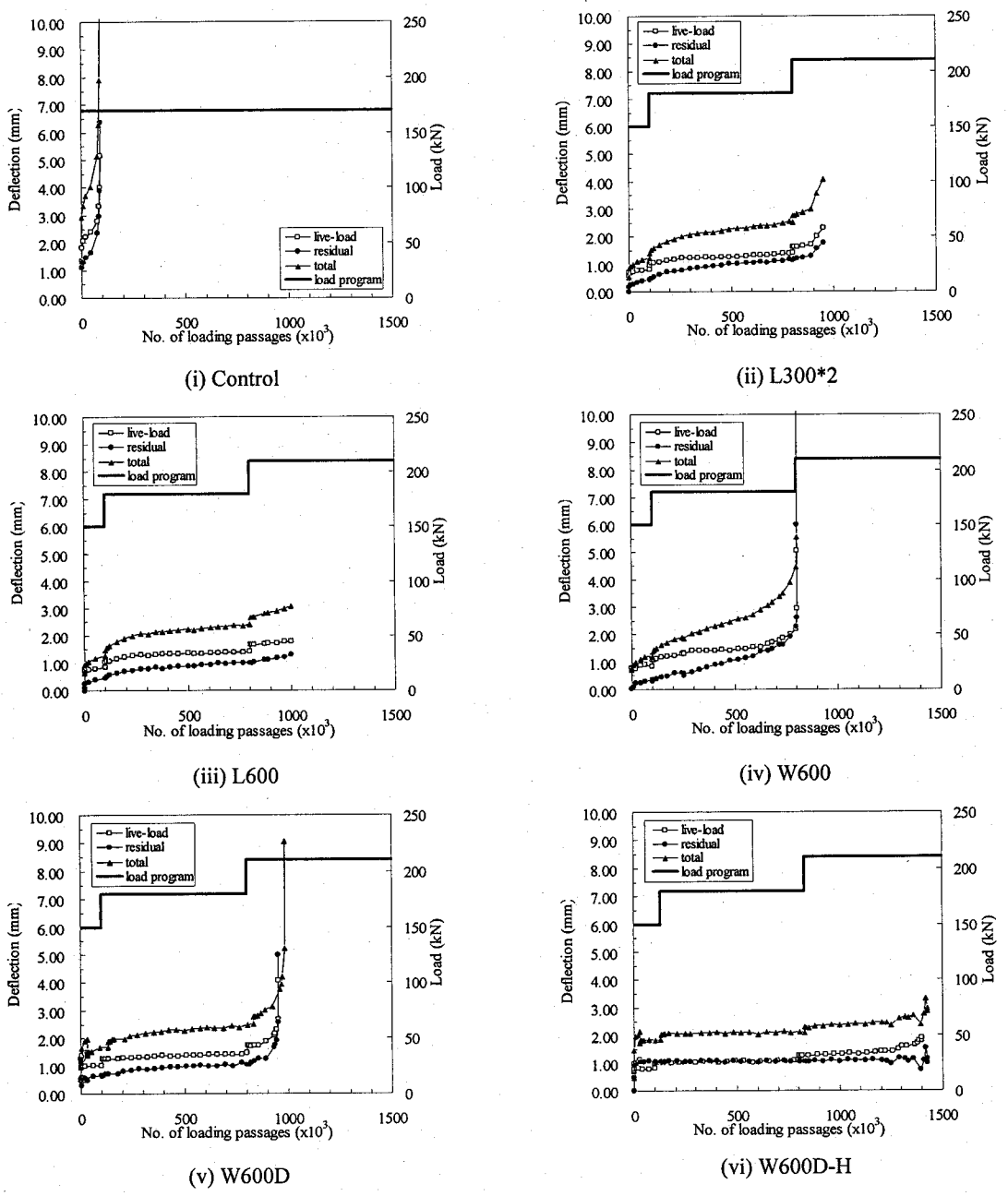

Fig. 16 Change of deflections

(ii) Change of deflections

The live-load deflections measured immediately after the strengthening for specimens W600D and W600D-H were 37.7% and 37.5% lower than those measured at the end of the preliminary loading, respectively. The change of mid-span deflections is given in Fig. 16. The residual deflection indicates the permanent deformation of specimens as a result of fatigue deterioration. The live-load deflection shows the elastic behavior of specimen when loaded statically, and is highly influenced by the flexural rigidity of the specimens as a plate structure. The total deflection is the sum of the residual and live-load deflections. Among the specimens which were strengthened with the warp-knitted type CFRP sheets, specimen W600D and W600D-H marked a stable development in deflections when compared to specimen W600. When the deflection results of the specimens strengthened with the warp-knitted type CFRP sheets are compared with that of the specimens strengthened with the laminated type CFRP sheets, it is found that specimen W600D, which has lower concrete elastic modulus, exhibited equivalent stiffness to that of specimens L300*2 and L600. Specimen W600D eventually

failed with N_f very close to that of specimen L300*2.

(iii) Debonding of CFRP sheets

Experimental observations revealed that debonding of the CFRP sheets occurred only at the final stages of the fatigue tests, at time when the punching shear has developed extensively. Due to the vertical movements of the crack surfaces, separation of the CFRP sheets from the concrete surface occurred. Examples of debonding patterns are shown in Fig. 17. Similar debonding patterns were observed for both types of CFRP sheets. Fig. 18 shows the distributing bar cross sectional of a strengthened slab which failed by punching shear. The debonding area was in fact located at the bottom the diagonal shear cracks and their vicinity area.

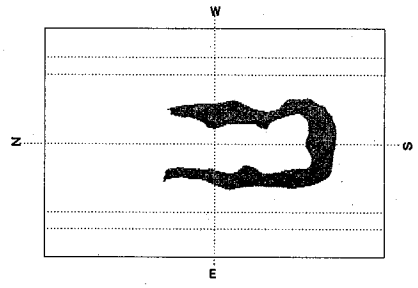

(i) L300*2

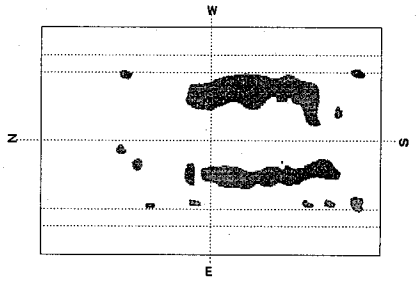

(ii) W600-D

Fig. 17 Debonding of CFRP

3.3 Fatigue lifespan extension

In order to evaluate the fatigue lifespan extension due to the strengthening by CFRP sheets, it is essential to predict the lifespan of the relevant specimens under unstrengthened condition. Matsui [8] proposed the following *S-N* equation that is widely used to estimate the fatigue lifespan of ordinary RC deck slabs:

$$\log(P/P_{sx}) = -0.07835 \log N_f + \log 1.520 \qquad (2)$$

where P is the applied load and P_{sx} is the punching shear strength for fatigue failure of RC slabs. In the experimental program for the strengthened specimens, the fatigue load was increased stepwise. Hence the calculation for the total number of equivalent loading passages under one reference load, N_{eq} is required by adopting the following:

$$N_f = N_{eq} = \sum (P_i/P)^{1/m} \cdot N_i \qquad (3)$$

where P_i is the load in respective loading stages, N_i is the total loading passages that corresponds with P_i and m is the gradient of the *S-N* equation as given in Equation (2). By taking P as 150kN, N_f of the specimens under unstrengthened condition were calculated with Equation (2). Under strengthened conditions, N_f of the specimens taken from the experimental results were converted by employing Equation (3). Lifespan extension, α_a was taken as the ratio between N_f of the specimens under strengthened condition and that under unstrengthened condition. The computed results are shown in

Table 5 Lifespan extension ratio

Specimen	N_f at 150kN (x10^3)		α_a	α_b
	(I)	(II)		
Control	-	454	-	1.0
L300*2	595	14,455	24.3	31.8
L600	595	17,319	>29.1	>38.1
W600	750	7,570	10.1	16.7
W600D	740	18,520	25.0	40.8
W600D-H	1,130	51,051	45.2	112.4

(I): Unstrengthened conditions, based on calculations by Equation (2)
(II): Strengthened conditions except Control, based on conversions of experimental results by Equation (3)

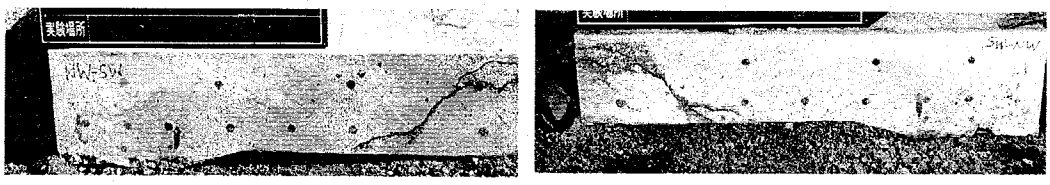

Fig. 18 Shear cracks on distributing bar cross section

Table 5. The lifespan extension ratio, α_b of the strengthened specimens were compared with that of the control specimen, α_b of more than 30 can be obtained except for specimen W600. This suggests that the high-fiber-density CFRP sheets are as effective as those with lower fiber density but higher elastic modulus in ensuring sufficient lifespan extension of RC slabs subjected to fatigue load. Although specimen W600 has the lowest α_a and α_b among all, the strengthening performance of the warp-knitted CFRP sheets is considered to be at least equivalent to that of the laminated type CFRP sheets. Furthermore, the static and fatigue bond test results also suggests high strengthening performance of the warp-knitted type CFRP sheets based on excellent bond strength and bond durability.

4. Conclusions

The main conclusions are summarized as follows:

1) Specimens bonded with one layer of the 600g/m^2 warp-knitted type CFRP sheet has bond strength of approximately 28% higher than that bonded with 2 layers of the 300g/m^2 laminated type CFRP sheets. This shows that despite similar strengthening volume, a more effective transfer of stresses can be anticipated in one layer of the 600g/m^2 warp-knitted type CFRP sheet relative to 2 layers of the 300g/m^2 laminated type CFRP sheets.
2) Under repeated load, excellent fatigue durability of the bond by one layer of the 600g/m^2 warp-knitted type CFRP sheet is verified, in which the fatigue cycles is approximately 3.3~5.0 times that of the bond by two layers of the 300g/m^2 laminated type CFRP sheets.
3) When the CFRP sheets are used to strengthen RC slabs to extend their fatigue durability, the 600g/m^2 high-fiber-density CFRP sheets, regardless of knit structures exhibit excellent strengthening performance with lifespan extension of slabs at least equivalent to that of slabs bonded with 2 layers of the 300g/m^2 laminated type CFRP sheets.

Acknowledgements

The financial support from Maeda Kosen Co. Ltd. is gratefully acknowledged. Assistance from all students of the laboratory during the experimental works is also greatly appreciated.

References

1) Sakai, H., Otaguro, H., Hisabe, N., Hoshijima, T., Ando, T. and Matsui, S., Experimental study on strengthening of high-modulus carbon fiber on damaged concrete deck slab, *Proceedings of the Development in Short and Medium Span Bridge Engineering 98*, CSCE, Calgary, Canada, pp.475-486, 1998.
2) Mori, N., Wakashita, F., Matsui, S. and Nishikawa, K., Reinforcing effect of carbon fiber sheets on damaged bridge slab, *Bridge and Foundation Engineering*, 95-3, pp.41-48, 1995.
3) Takai, T., Matsui, S. and Hayashida, M., Research on the strengthening of deck slabs by CFRP sheet, *Proceedings of the Annual Conference of Civil Engineers*, JSCE, I-A185, pp.368-369, 1997.
4) Okada, M., Onishi, H., Matsui, S. and Kobayashi, A., Stiffening effect with CFRP sheets arranged in grid pattern on RC decks, *Proceedings of The 3rd Symposium on Decks of Highway Bridge*, JSCE, pp.175-180, 2003.
5) Teng, J. G., Chen, J. F., Smith, S. T. and Lam, L., *FRP-strengthened RC structures*, John Wiley & Sons Ltd., England, pp.245, 2000.
6) Shen, H. S., Teng, J. G. and Yang, J., Interfacial stresses in beams and slabs bonded with thin plates, *Journal of Engineering Mechanics*, ASCE, Vol. 127, No. 4, pp.399-406, 2001.
7) Maalej, M. and Bian, Y., Interfacial shear concentration in FRP-strengthened beams, *Composite Structures*, Vol. 54, No.4, pp.417-426, 2001.
8) Matsui, S., Prediction of bridge lifespan- Fatigue lifespan prediction of RC decks of highway bridges, *Safety Engineering*, Vol. 30, No. 6, pp.432-440, 1991.